

From the RSNA Refresher Courses

State-of-the-Art Adrenal Imaging¹

CME FEATURE

See accompanying
test at [http://
www.rsna.org/
education/
rg_cme.html](http://www.rsna.org/education/rg_cme.html)

William W. Mayo-Smith, MD • Giles W. Boland, MD • Richard B. Noto, MD • Michael J. Lee, MD

LEARNING OBJECTIVES FOR TEST 6

*After reading this
article and taking
the test, the reader
will be able to:*

- Differentiate adrenal adenomas from metastases at nonenhanced CT.
- Describe the enhancement patterns of adenomas and metastases.
- Differentiate adrenal masses based on CT and MR imaging features.
- Describe the appropriate radiologic work-up of a suspected pheochromocytoma.
- Describe three different CT techniques for performing an adrenal biopsy.

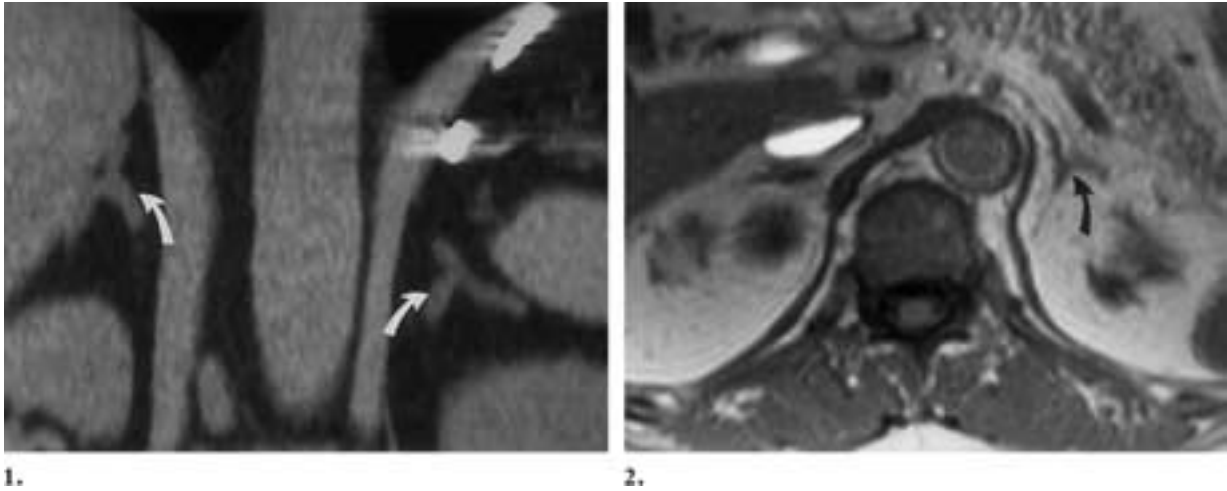
The adrenal gland is a common site of disease, and detection of adrenal masses has increased with the expanding use of cross-sectional imaging. Radiology is playing a critical role in not only the detection of adrenal abnormalities but in characterizing them as benign or malignant. The purpose of the article is to illustrate and describe the appropriate radiologic work-up for diseases affecting the adrenal gland. The work-up of a suspected hyperfunctioning adrenal mass (pheochromocytoma and aldosteronoma) should start with appropriate biochemical screening tests followed by thin-collimation computed tomography (CT). If results of CT are not diagnostic, magnetic resonance (MR) and nuclear medicine imaging examinations should be performed. CT has become the study of choice to differentiate a benign adenoma from a metastasis in the oncology patient. If the attenuation of the adrenal gland is over 10 HU at nonenhanced CT, contrast material-enhanced CT should be performed and washout calculated. Over 50% washout of contrast material on a 10-minute delayed CT scan is diagnostic of an adenoma. For adrenal lesions that are indeterminate at CT in the oncology patient, chemical shift MR imaging or adrenal biopsy should be performed. Certain features can be used by the radiologist to establish a definitive diagnosis for most adrenal masses (including carcinoma, infections, and hemorrhage) based on imaging findings alone.

Abbreviations: ACTH = adrenocorticotropic hormone, MIBG = meta-iodobenzylguanidine, NP-59 = iodine-131 6-beta-iodomethyl-19-norcholesterol, PET = positron emission tomography

Index terms: Adrenal gland, biopsy, 86.1261 • Adrenal gland, CT, 86.1211 • Adrenal gland, MR, 86.121414 • Adrenal gland, neoplasms, 86.317, 86.328, 86.33

RadioGraphics 2001; 21:995–1012

¹From the Departments of Radiology of Brown University, Rhode Island Hospital, 593 Eddy St, Providence, RI 02903 (W.W.M.-S., R.B.N.); Harvard University, Massachusetts General Hospital, Boston, Mass (G.W.B.); and Royal College of Surgeons, Beaumont Hospital, Dublin, Ireland (M.J.L.). Received October 25, 2000; revision requested November 15 and received December 28; accepted December 29. **Address correspondence to** W.W.M.-S. (e-mail: william_mayo-smith@brown.edu).



Figures 1, 2. Normal adrenal gland. (1) Coronal reformatted image from helical CT data shows the triangular shape of the adrenal gland (arrows) and its relationship to the kidneys and diaphragms. (2) T1-weighted breath-hold MR image demonstrates a normal left adrenal gland (arrow).

I am unaware that any modern authority has ventured to assign to them any special function or influence whatever.

Thomas Addison, 1855

Introduction

Remarkable progress has been made in elucidating the structure and function of the adrenal gland since the time of Thomas Addison. More recently, a large amount of radiologic research has been performed on both the detection and characterization of adrenal abnormalities. The purpose of this article is to (a) give an overview of adrenal diseases and their imaging appearances, (b) describe the current concepts of differentiating a benign from a malignant adrenal mass with particular attention to computed tomography (CT) and magnetic resonance (MR) imaging, (c) describe techniques of adrenal biopsy, and (d) present an imaging algorithm for characterizing an adrenal mass.

The adrenal gland is named for its location adjacent to the kidneys: ad-renal. The normal gland weighs 5 g and has a characteristic inverted Y, V, or T shape (Figs 1, 2). The adrenal gland is made of cortex that is derived from the mesoderm and medulla derived from the neural crest. The adrenal cortex secretes cortisol, aldosterone, and androgens, and the medulla secretes epinephrine and norepinephrine. The adrenal gland is routinely identified at abdominal CT and MR imaging examinations (1).

Abnormalities of the adrenal gland include primary neoplasm, metastases, hemorrhage, or enlargement of the adrenal gland from external hor-

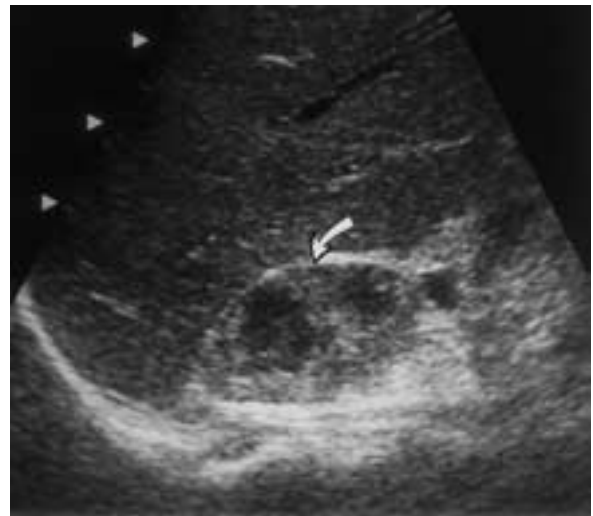


Figure 3. Sagittal US scan demonstrates an enlarged right adrenal gland (arrow) lying posterior to the right lobe of the liver. Although US may reveal adrenal masses, CT is the modality of choice for initial adrenal mass characterization.

monal stimulation. Adrenal masses can be divided into two physiologic categories based on whether they hypersecrete a hormone. Hyperfunctioning adrenal masses produce a hormone that results in a chemical imbalance and include pheochromocytomas, aldosteronomas, and cortisol or androgen-producing tumors. Nonfunctioning adrenal masses cause enlargement of the adrenal gland but no significant increased hormone production. Adrenal adenomas and metastases are the most common nonfunctioning adrenal masses.

There are numerous imaging modalities including CT, MR imaging, ultrasonography (US), and nuclear medicine imaging that can be used to evaluate the adrenal gland (Fig 3). CT is the pri-

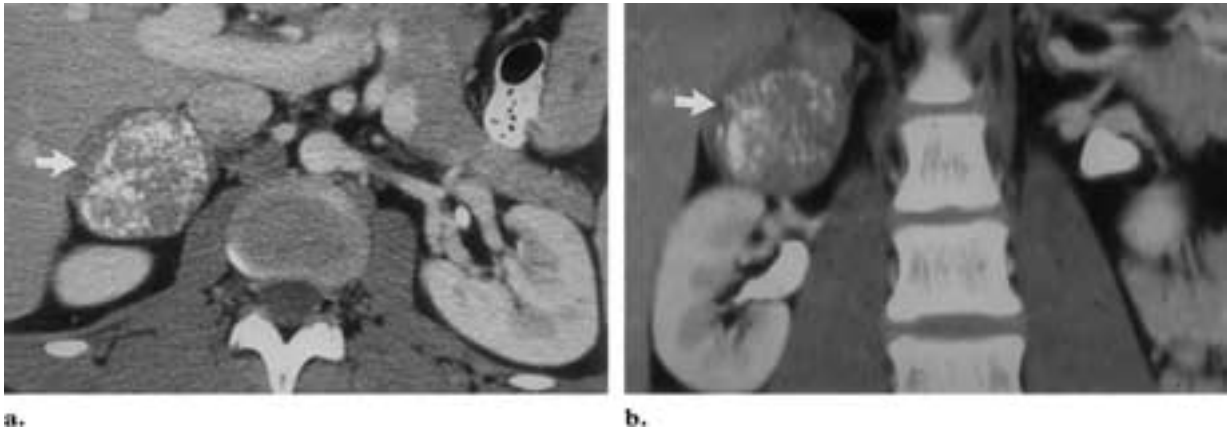


Figure 4. Pheochromocytoma in a 30-year-old man evaluated with CT. **(a)** Contrast-enhanced axial CT scan demonstrates an enlarged right adrenal gland with internal calcifications (arrow). **(b)** Coronal reformatted image from the axial data set demonstrates the relationship of the right adrenal pheochromocytoma (arrow) to the upper pole of the right kidney and the liver.

primary modality for both detection and characterization of adrenal masses. If an adrenal mass is suspected, CT technique should be tailored to optimize visualization of the adrenal gland. We recommend use of 3-mm helical collimation with the field of view targeted to the adrenal gland. A nonenhanced examination should be performed followed by a contrast material-enhanced study if necessary, as described later in this article.

Chemical shift MR imaging is useful as a problem-solving modality when evaluating the adrenal gland, and T2-weighted imaging may be helpful for detecting a pheochromocytoma. Nuclear medicine imaging is primarily a problem-solving modality for lesions not adequately characterized with CT and MR imaging. Iodine-131 meta-iodobenzylguanidine (MIBG) and indium-111 octreotide are used to evaluate for pheochromocytoma, and I-131 6-beta-iodomethyl-19-nor-cholesterol (NP-59) can be used to detect aldosteronomas and other hyperfunctioning cortical tumors. Positron emission tomography (PET) shows promise in differentiating benign from malignant masses.

Hyperfunctioning Adrenal Neoplasms

Hyperfunctioning diseases of the adrenal gland originate from either the adrenal medulla (pheochromocytoma) or the adrenal cortex (Cushing syndrome, Conn syndrome, or hyperandrogenism). The clinical sequelae depend on the type of hormone produced and its target organs.

Hyperfunctioning Adrenal Medullary Neoplasms

Pheochromocytoma is a neoplasm of the adrenal medulla. Although they are typically unilateral and benign, pheochromocytomas may be bilateral and malignant in 10% of patients (3). The tumor secretes catecholamines that can result in hypertension and palpitations. The clinical diagnosis is suspected in a younger patient with hypertension. The first-line tests for evaluating a patient with suspected pheochromocytoma are plasma catecholamine levels and 24-hour urine vanillylmandelic acid and metanephrine levels. These tests have sensitivities ranging from 89% to 100%, although false-negative values may result from exogenous drugs or episodic catecholamine production (2). Although hypertension is one of the most common symptoms of pheochromocytoma, pheochromocytomas are the cause of hypertension in less than 1% of hypertensive patients.

When a pheochromocytoma is suspected on clinical and laboratory grounds, CT is the study of choice to confirm the diagnosis. Typically, an adrenal mass is identified at CT (Fig 4). Three-dimensional imaging and coronal reconstructions may be helpful to demonstrate adjacent vessels, particularly with the recent advent of laparoscopic adrenalectomy (4). If an adrenal mass is identified at CT in a patient with a suspected pheochromocytoma, the treatment is surgical resection. If an



Figure 5. Pheochromocytoma in a 45-year-old woman evaluated with MR imaging. **(a)** Axial T2-weighted image with fat saturation demonstrates a bright mass in the right adrenal gland (arrow). **(b)** Coronal T2-weighted image with fat saturation helps confirm the location of the mass in the adrenal gland (arrow) and that it is separate from the liver and the kidney.

adrenal mass is not seen, attention should be directed to the paraspinous region because 10% of pheochromocytomas are extraadrenal. Paraganglioma is the preferred term for such tumors, rather than extraadrenal pheochromocytoma.

The MR imaging appearance of a pheochromocytoma has typically been described as T2 hyperintense (Fig 5); however, not all pheochromocytomas have this imaging characteristic (5,6). MR imaging is useful for detecting extraadrenal paragangliomas and recurrences after resection, given their increased signal intensity on T2-weighted images.

For patients in whom a pheochromocytoma is suspected and an adrenal mass is not identified at CT or MR imaging, nuclear medicine imaging can be used. I-131 MIBG and In-111 octreotide are the two radiopharmaceuticals used to evaluate for a pheochromocytoma. I-131 MIBG is a structural analog of norepinephrine, which is stored in neurosecretory granules of the adrenal medulla. Abdominal imaging is performed 24–72 hours after administration of the agent, and whole-body imaging should be performed to detect extraadrenal lesions. If there is a high clinical suspicion of a perivesicular paraganglioma, bladder catheterization may be necessary as the agent is excreted in the urine. When pheochromocytoma is suspected, any focal uptake of I-131 MIBG in the adrenal gland is abnormal (Fig 6). The reported sensitivity of I-131 MIBG for detection of a pheochromocytoma is 80%–90%, with a specificity of 90%–100% (7–9). I-131 MIBG scintigraphy is useful to detect the 10% of pheochromocytomas

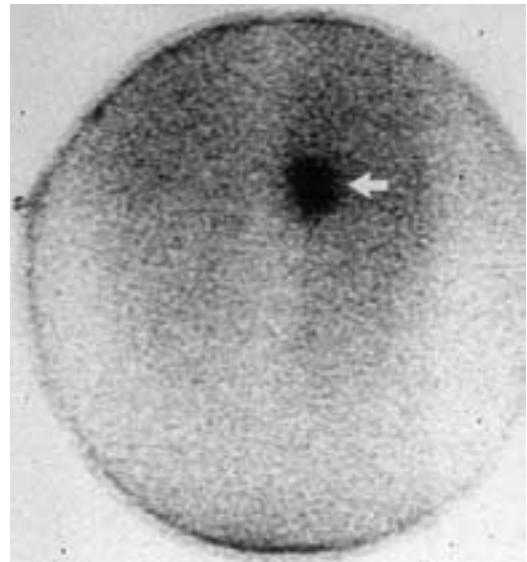


Figure 6. Pheochromocytoma in a patient evaluated with nuclear medicine imaging. Posterior image obtained 48 hours after intravenous administration of I-131 MIBG demonstrates increased activity in the right adrenal gland (arrow).

that are extraadrenal and to document metastatic disease or residual tumor after surgery.

In-111 octreotide, the second agent used to detect pheochromocytomas, is a synthetic octapeptide analog of somatostatin that shows uptake in a variety of tumors that contain somatostatin receptors. A total of 5 mCi (185 MBq) of In-111 octreotide is administered intravenously, and whole-body imaging is performed at 4 and 24 hours after injection. In-111 octreotide has a sensitivity of 75%–90% for detection of pheochro-



Figure 7. Adrenal hyperplasia in a woman with Cushing disease. Contrast-enhanced CT scan demonstrates thickening of the limbs of the left adrenal gland but a normal right adrenal gland. The prominent intra-abdominal fat and hepatic steatosis seen here are typical findings in this disease.

mocytomas (10). There is a complementary role for In-111 octreotide and I-131 MIBG, since 25% of pheochromocytomas are seen only with I-131 MIBG and another 25% are seen only with In-111 octreotide. The remaining 50% of pheochromocytomas are visualized with both agents.

Hyperfunctioning Adrenal Cortical Neoplasms

The adrenal cortex is composed of three separate zones: the zona fasciculata, the zona glomerulosa, and the zona reticularis. The zona fasciculata produces cortisol, the zona glomerulosa produces aldosterone, and the zona reticularis produces androgens. All three are produced in response to adrenocorticotrophic hormone (ACTH) produced by the pituitary gland; however, only cortisol has negative feedback on ACTH production (11). Hyperfunctioning tumors of the adrenal cortex can produce Cushing syndrome from cortisol overproduction, Conn syndrome from production of aldosterone, or hyperandrogenism from overproduction of androgens.

Cushing Syndrome.—Cushing syndrome is defined as increased glucocorticoid levels from any cause and may be divided into ACTH-dependent and ACTH-independent forms. In Cushing disease, which accounts for approximately 80% of Cushing syndrome cases, a pituitary adenoma secretes excess ACTH, which stimulates the adrenal gland.

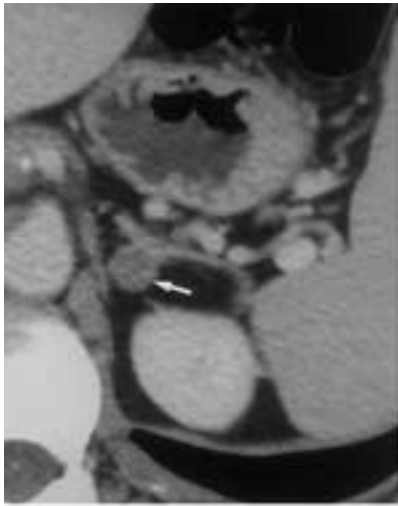
Appropriate work-up of patients with suspected Cushing disease includes measurement of serum ACTH levels, a dexamethasone suppression test, and pituitary MR imaging. The adrenal glands are often symmetrically enlarged in patients with ACTH-dependent Cushing syndrome; however, up to 30% of patients will have normal-size adrenal glands (12) (Fig 7). In 15%–25% of cases of Cushing syndrome, the cause is a primary adrenal neoplasm, usually a benign adenoma (13). Adrenal adenomas causing Cushing syndrome are usually greater than 2.0 cm in diameter and often readily visualized on CT scans. The role of scintigraphy for the evaluation of patients with Cushing syndrome is limited, particularly with the advances in CT and MR imaging. Adrenal cortical scintigraphy is sensitive for localization of adrenal remnants in patients who have persistent elevated cortisol levels after adrenalectomy (14).

Hyperaldosteronism.—Primary aldosteronism is characterized clinically by hypertension and hypokalemia. The cause is an adrenal adenoma in about 80% of patients and adrenal gland hyperplasia in 20% (15). Adrenal carcinoma is an extremely rare cause of primary aldosteronism.

After the diagnosis of hyperaldosteronism has been established through clinical and laboratory tests, a dedicated CT study of the adrenal gland performed with thin (3-mm) collimation is usually the first-line imaging examination (Fig 8). Adrenal adenomas are often small and difficult to detect, since over 20% are less than 1 cm in diameter (16).

Adrenal cortical scintigraphy is rarely needed, given the improvements in CT technology, but it can be useful to determine whether the abnormality is unilateral or bilateral (17). NP-59 is a cholesterol analog that binds to the low-density lipoprotein receptors of the adrenal cortex and is the primary radiopharmaceutical used for adrenal cortical scintigraphy. It is available only through the University of Michigan (Ann Arbor) radiopharmacy and is still considered investigational by the U.S. Food and Drug Administration despite many years of safe use. A normal result of NP-59 imaging is visualization of both adrenal glands on day 5 after the injection or thereafter. Bilateral early adrenal visualization before day 5 suggests adrenal gland hyperplasia. Unilateral early adrenal visualization before day 5 is indicative of an

Figures 8–10. (8) Left adrenal aldosteronoma in a 43-year-old woman. Contrast-enhanced helical CT scan shows a 5-mm well-circumscribed left adrenal mass (arrow), which proved at surgery to be an aldosterone-secreting adenoma. (9) Functioning right aldosteronoma in a patient with hyperaldosteronism. Posterior image obtained 5 days after intravenous administration of NP-59 shows increased activity in the right adrenal gland (arrow), a finding consistent with a functioning adenoma. Normal activity is seen in the bowel, bladder, and liver. (10) Adrenal venous sampling in a 51-year-old man with biochemically proved aldosteronoma. Angiogram shows the catheter, which was placed in the right adrenal vein (arrow) via the inferior vena cava. The adrenal veins were opacified by using gentle hand injection of contrast material, thus confirming correct placement for adrenal venous sampling. Cortrosyn-stimulated aldosterone levels were four times higher on the left than the right. The patient's symptoms resolved after left adrenalectomy.



8.



9.



10.

adenoma (Fig 9). If these examinations are not diagnostic, adrenal venous sampling should be performed (Fig 10) to determine whether aldosterone secretion lateralizes to one side (suggestive of an adenoma) or is symmetric (suggestive of bilateral hyperplasia).

Characterization of an Adrenal Mass: Is It Benign or Malignant?

Adrenal masses are common, estimated to occur in 9% of the population (18,19). However, the adrenal gland is also a common site of metastasis, particularly from lung carcinoma. With the proliferation of cross-sectional imaging, detection of an incidental adrenal mass has become a common problem. In patients with no known primary cancer, an adrenal mass is almost always a benign adenoma. However, in a patient with a known neoplasm, particularly lung cancer, the finding of an adrenal mass is problematic, since metastasis to the adrenal gland indicates advanced disease that is not amenable to surgical resection and potential cure. Thus, differentiating an adrenal mass as benign or malignant is critical in the oncology patient, since it will greatly affect patient treat-

ment and prognosis. One study has shown that 27% of oncology patients have microscopic adrenal metastases (20). When the imaging task is differentiating an adenoma from metastasis, the high specificity of the modality used is critical (21). Herein, we discuss the use of nonenhanced CT, contrast-enhanced CT, MR imaging, and PET to characterize adrenal masses in the oncology patient.

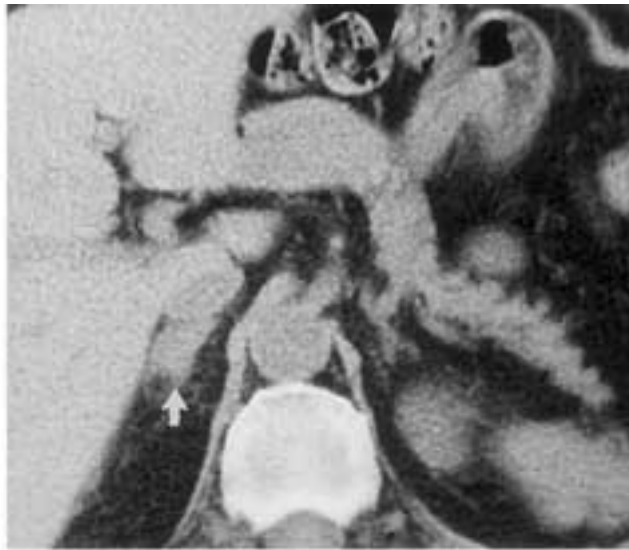
CT in Differentiating Benign from Malignant Adrenal Masses

At CT, certain imaging findings are helpful in differentiating benign from malignant lesions. Larger lesions have a greater likelihood of being malignant. In particular, lesions greater than 4 cm in diameter tend to be either metastasis or a primary adrenal carcinoma. Change in lesion size is a useful indicator of malignancy because adenomas are slow growing and tend not to change size. The shape of the adrenal gland can also be helpful in predicting malignancy. Adenomas tend to have smooth margins and a homogeneous density, whereas metastases can be heterogeneous and have an irregular shape. However, although these findings are helpful in differentiating a benign

Figures 11, 12. (11) Typical nonenhanced CT findings of an adrenal adenoma in a 64-year-old man with no known malignancy. The left adrenal adenoma (arrow) has smooth margins, is well defined, and has an attenuation of 5 HU, all findings characteristic of an adenoma. (12) Typical nonenhanced helical CT findings of metastasis in a 76-year-old man with lung carcinoma. On the CT scan, the right adrenal gland (arrow) is enlarged, has irregular contours, and has an attenuation of 36 HU, all findings characteristic of metastasis. Adrenal masses with attenuation values over 10 HU at nonenhanced CT require further evaluation with either CT contrast material washout, chemical shift MR imaging, or adrenal biopsy.



11.



12.

from a malignant adrenal mass, they are not specific.

Currently, there are two main CT criteria (histologic and physiologic) used to differentiate benign adenomas from malignant adrenal masses. Intracellular lipid content of the adrenal mass represents the anatomic difference between adenomas and metastases, and differences in vascular enhancement patterns represent the physiologic difference. Adenomas have abundant intracytoplasmic fat in the adrenal cortex and thus have low attenuation at CT (Fig 11). Conversely, metastases have little intracytoplasmic fat and thus do not have low attenuation at nonenhanced CT (Fig 12). Korobkin et al (22) performed a study quantifying adrenal fat and showed a high correlation between adrenal fat content and low attenuation at CT and signal loss at chemical shift MR imaging.

Nonenhanced CT.—The first study to use nonenhanced CT to characterize adrenal masses as benign and malignant was performed by Lee et al (23). In this study, the mean attenuation of adenomas was -2.2 HU and metastasis was 29 HU. At a threshold of 0 HU, the sensitivity of nonenhanced CT for characterizing adrenal adenomas was 47%, with a specificity of 100%. At a threshold of 10 HU, the sensitivity changed to 79%, with a specificity of 96%. Subsequent studies have corroborated these findings (24,25). Thresholds to differentiate benign from malig-

nant lesions have ranged from 0 to 18 HU. Bolland et al (25) performed a meta-analysis of 10 studies to determine an optimal threshold for differentiating benign from malignant lesions. From this study, a threshold of 10 HU had a 71% sensitivity and 98% specificity for characterizing adrenal masses. This specificity approached 100% when other features such as adrenal size, shape, and change in lesion size were considered. When measuring the attenuation of the adrenal gland, it is important to use as large a region of interest as possible to fill the gland but to not include adjacent perirenal fat.

Contrast-enhanced CT.—Although the finding of lower attenuation is useful to characterize an adenoma, it is estimated that up to 30% of adenomas do not contain sufficient lipid to have low attenuation at CT (26,27). The problem is that adenomas represent a heterogeneous population: Approximately 70% of them have intracellular lipid but 30% do not. Thus, although nonenhanced CT can be used to identify 70% of adenomas, it does not allow the 30% that do not contain lipid to be reliably differentiated from metastases. In addition, although nonenhanced CT is useful to differentiate adenomas from metastases, the majority of CT examinations in oncology patients use intravenous contrast material.



Figure 13. Typical attenuation and washout of intravenous contrast material in a left adrenal adenoma in a 54-year-old woman with a history of breast carcinoma. **(a)** Nonenhanced CT scan shows a left adrenal adenoma (arrow), which has an attenuation of 4 HU. **(b)** On the dynamic enhanced phase image, the adrenal gland (arrow) enhances vigorously to 54 HU. **(c)** On the 10-minute delayed image, the attenuation of the left adrenal gland (arrow) is 23 HU (lower than that of the normal right adrenal gland, kidneys, and liver). There is greater than 50% washout between the dynamic phase of contrast enhancement and the 10-minute delay, which is diagnostic of an adenoma and confirms the finding on the nonenhanced CT scan. Quantitative region-of-interest measurements (in Hounsfield units) are important because degree of enhancement is difficult to quantify with the human eye.

The second imaging parameter to differentiate adenomas from metastases relies on physiologic differences in perfusion. Adenomas enhance rapidly with intravenous contrast media (either iodinated agents used at CT or gadolinium chelates used at MR imaging) and wash out the agent rapidly (Fig 13). Metastases also enhance vigorously with contrast material, but the washout of the agent is more prolonged than with adenomas (Fig 14). This difference in washout of contrast media has been exploited to further differentiate benign from malignant adrenal lesions.

Dynamic contrast-enhanced CT is usually performed in the portal venous phase of enhancement (60–80 seconds after starting the injection of contrast material). Although this timing is useful for detecting hepatic lesions, it is suboptimal for differentiating benign from malignant adrenal lesions because both adenomas and metastases



enhance early. Thus, the attenuation values of adenomas and metastases significantly overlap, and dynamic CT is not sensitive for differentiating between the two. However, if delayed images are obtained after the administration of contrast media, washout of the agent can be determined. Several studies have investigated the use of delayed CT to characterize adrenal lesions (27–32).

Two features can be measured at delayed CT: the attenuation value of the adrenal gland and the washout of contrast media. A Hounsfield unit of less than approximately 30 at 10 minutes after injection has been shown to be diagnostic of a lipid-rich adenoma; however, most adenomas have an attenuation value higher than 30, and thus it is a specific but not a sensitive test (30). A more useful parameter is the percentage of washout of contrast material in which the attenuation of the adrenal gland at delayed CT is compared

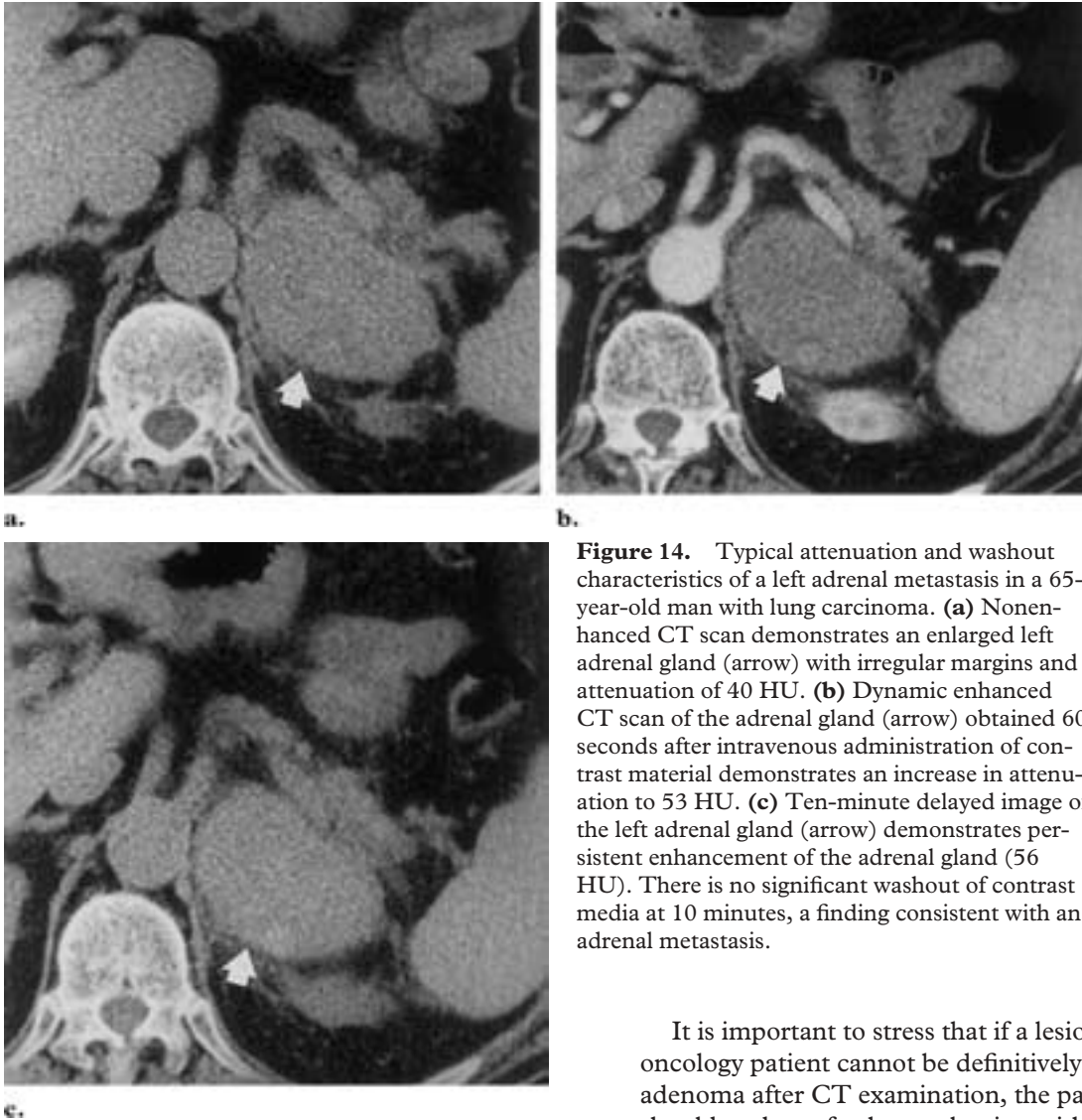


Figure 14. Typical attenuation and washout characteristics of a left adrenal metastasis in a 65-year-old man with lung carcinoma. **(a)** Nonenhanced CT scan demonstrates an enlarged left adrenal gland (arrow) with irregular margins and attenuation of 40 HU. **(b)** Dynamic enhanced CT scan of the adrenal gland (arrow) obtained 60 seconds after intravenous administration of contrast material demonstrates an increase in attenuation to 53 HU. **(c)** Ten-minute delayed image of the left adrenal gland (arrow) demonstrates persistent enhancement of the adrenal gland (56 HU). There is no significant washout of contrast media at 10 minutes, a finding consistent with an adrenal metastasis.

with its attenuation at dynamic CT. Loss of 50% of the attenuation value of the adrenal mass at delayed CT is specific for an adenoma; less than 50% washout is indicative of either a metastasis or an atypical adenoma. Percentage of washout is typically calculated by the following formula: $(1 - \text{delayed enhanced HU value}/\text{initial enhanced HU value}) \times 100$. Quantitative region-of-interest measurements (in Hounsfield units) are important because degree of enhancement is difficult to quantify with the human eye. Recently, Caoili et al (26) studied a group of adenomas that had elevated attenuation values at nonenhanced CT and thus could not be differentiated from metastasis based on nonenhanced CT findings. They found that this subset of adenomas demonstrated washout features typical of all adenomas. This study (corroborated by the work of Pena et al [27]) is exciting, since it demonstrates that washout of contrast media may be more specific than low attenuation at CT.

It is important to stress that if a lesion in an oncology patient cannot be definitively called an adenoma after CT examination, the patient should undergo further evaluation with MR imaging or an adrenal biopsy to confirm a benign or malignant adrenal lesion. Thus, although an attenuation value of less than 10 HU at nonenhanced CT is diagnostic of an adenoma, an attenuation value of greater than 10 HU is not diagnostic of a metastasis. A lesion greater than 10 HU at nonenhanced CT may be either an adenoma or metastasis.

MR Imaging in Differentiating Benign from Malignant Masses

Various MR imaging parameters can be used to characterize adrenal masses, including T1 and T2 characteristics, calculated T2 values, enhancement patterns, and chemical shift characteristics. In general, metastases and carcinomas contain larger amounts of fluid than adenomas and thus appear bright on T2-weighted images. However, there is significant overlap in T1 and T2 signal intensity between adenomas and metastases, and

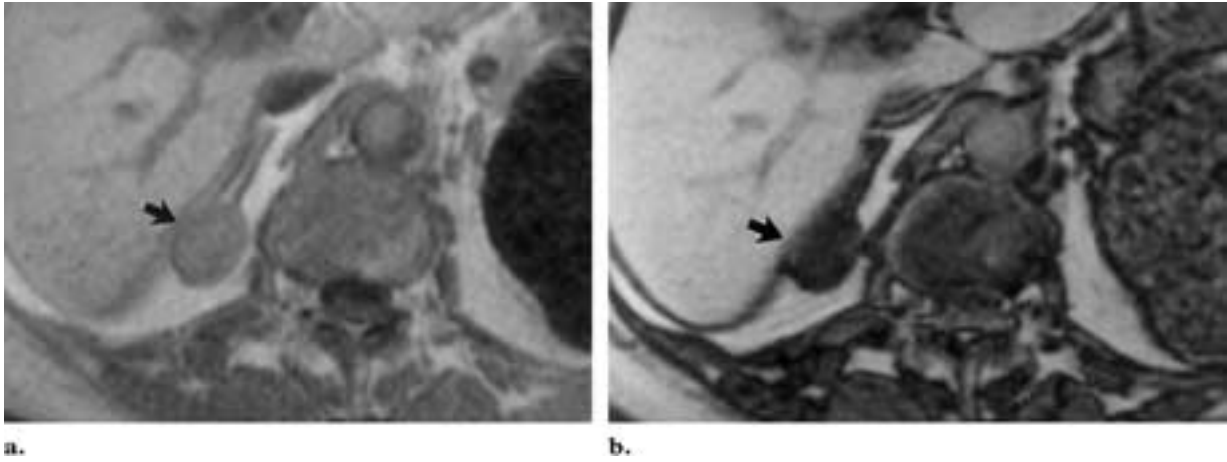


Figure 15. Indeterminate right adrenal mass found at CT in a 45-year-old woman with breast cancer. **(a)** T1-weighted in-phase MR image demonstrates a right adrenal mass (arrow). **(b)** T1-weighted out-of-phase MR image shows signal drop-off in the adrenal gland (arrow), which is diagnostic of an adenoma.

thus signal intensity is not useful to reliably differentiate between them. Enhancement patterns have also been investigated as a means of differentiating benign adrenal adenomas from metastases, and, similar to their appearance at CT, adenomas vigorously enhance and exhibit early washout of contrast material compared with metastases on MR images (33,34). Given the increased cost of MR imaging, CT is probably more cost effective to assess enhancement patterns. As stated earlier, intracellular lipid is high in most adrenal adenomas and low in metastases. Chemical shift imaging is an MR imaging technique used to detect lipid within an organ and is the most sensitive method for differentiating adenomas from metastases (35). In studies that have compared T1, T2, enhancement patterns, and chemical shift imaging for differentiating adenomas from metastases, the latter has demonstrated a high sensitivity and specificity (19,36–40).

Chemical shift imaging relies on the different resonance frequency rates of protons in fat and water molecules. The chemical environment of a proton in water is different than a proton in lipid because of the proximity of hydrogen and oxygen atoms and their electrons. Electrons surrounding the proton shield it from the applied external field. Thus, the effective magnetic field experienced by a shielded proton is less than that experienced by an unshielded proton. Fat protons are more shielded than water protons, experience less external magnetic field, and thus resonate at a slower frequency. It is this difference in resonance rate of protons in fat and water that is exploited in chemical shift imaging. The net effect of this physical phenomenon is that there is cancellation

of signal between lipid and water protons within a voxel. Thus, tissues containing lipid and water have signal loss (ie, appear darker) on out-of-phase images. Two studies have shown that the amount of signal drop-off within a voxel depends on the amount of lipid in the tissue (22,41).

To obtain chemical shift images, two breath-hold T1-weighted acquisitions are performed. The first uses a short echo time (2.2 msec at 1.5 T) when the fat and water protons are out of phase, and a second in-phase acquisition uses a longer echo time (4.4 msec). The echo time chosen to obtain in-phase and out-of-phase images varies as a function of field strength. On out-of-phase images, there is signal drop-off in adenomas due to the intra-voxel signal cancellation of the lipid and water protons. Thus, on out-of-phase images, the adenoma appears darker than on in-phase images (Fig 15). In adrenal masses that do not contain lipid (eg, metastases), there is no significant signal loss on out-of-phase images, and thus the signal intensity of the adrenal gland is the same on in-phase and out-of-phase images (Fig 16). With the chemical shift technique, the sensitivity and specificity for differentiating adenomas from metastases ranges from 81% to 100% and 94% to 100%, respectively (42–47).

When in-phase and out-of-phase images are compared, an internal standard is useful to visually quantify signal drop-off. In general, the liver is a less reliable internal standard because intrinsic liver disease (eg, steatosis, hemochromatosis) can cause variable hepatic signal intensity on in-phase and out-of-phase images (Fig 17). We find it useful to compare signal intensity of the adrenal gland with that of the spleen as the internal standard (42). It is also helpful for the technologists to use one prescan value for both in-phase and out-of-phase acquisitions, since variable prescan values can vary the signal intensity of the adrenal

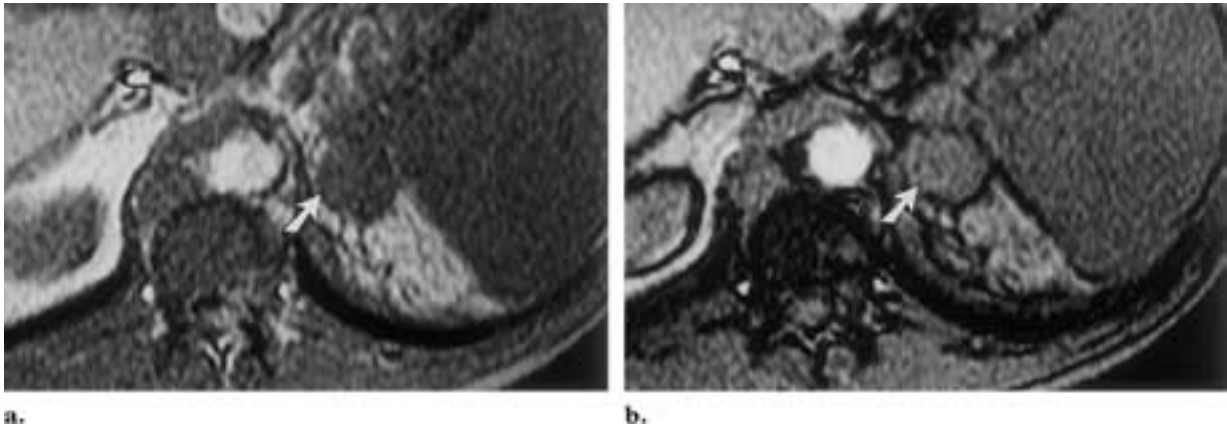


Figure 16. Left adrenal metastases in a 74-year-old man with lung cancer. **(a)** T1-weighted in-phase MR image demonstrates a left adrenal mass (arrow). **(b)** T1-weighted out-of-phase MR image shows no significant signal loss in the adrenal gland compared with that of the spleen. The mass is either a metastasis or atypical adenoma, and biopsy was recommended.

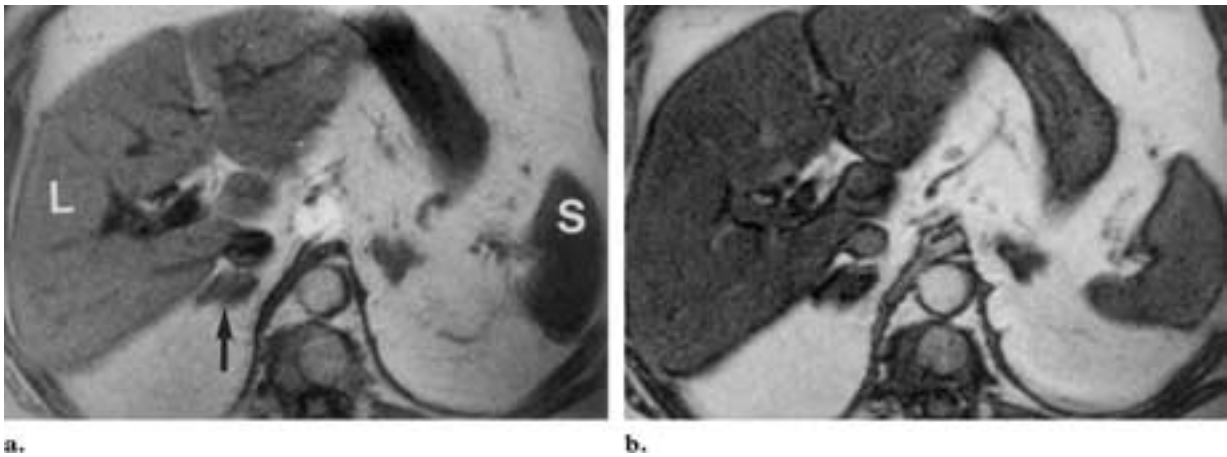


Figure 17. Right adrenal adenoma in a patient with hepatic steatosis. **(a)** T1-weighted in-phase MR image demonstrates a right adrenal mass (arrow), which is isointense relative to the liver (*L*) and slightly higher in signal intensity than the spleen (*S*). **(b)** T1-weighted out-of-phase MR image shows signal drop-off in both the liver (due to steatosis) and the mass. The adrenal mass has clearly lost signal compared with the spleen on out-of-phase images, a finding that is diagnostic of an adenoma.

gland. Finally, it is important for the technologist to use the same window and level values on both in-phase and out-of-phase images.

Collision tumors are rare entities that result when a metastasis occurs in an adrenal gland that has a pre-existing adrenal adenoma (48). In this circumstance, signal intensity for each tissue type matches that expected for each pulse sequence. Thus, the adenomatous portion of the adrenal gland loses signal on out-of-phase images and a metastasis does not.

In summary, chemical shift MR imaging is the most sensitive technique for differentiating adenomas from metastases to the adrenal gland. When results of CT examinations are equivocal, MR imaging is the next imaging study of choice for characterizing adrenal lesions (49). One study has shown that MR imaging is more cost-effective than performing biopsies in all equivocal adrenal lesions (50). However, given the most recent CT

literature, the role of MR imaging may be more limited since CT is more readily available and less expensive and as CT algorithms become refined.

PET in Differentiating Benign from Malignant Masses

More recently, PET has been suggested as a useful tool in the evaluation of the nonhyperfunctioning adrenal mass. Although still preliminary, the results of multiple recent studies suggest that PET performed with fluorine-18 fluorodeoxyglucose (FDG) is highly accurate in differentiating benign from malignant lesions. In general, malignant masses in the adrenal gland (and elsewhere) show increased uptake of FDG due to increased glucose utilization, but benign noninflammatory lesions show no evidence of increased FDG uptake (Figs 18, 19). Three recent studies demonstrated that FDG PET had 100% sensitivity and

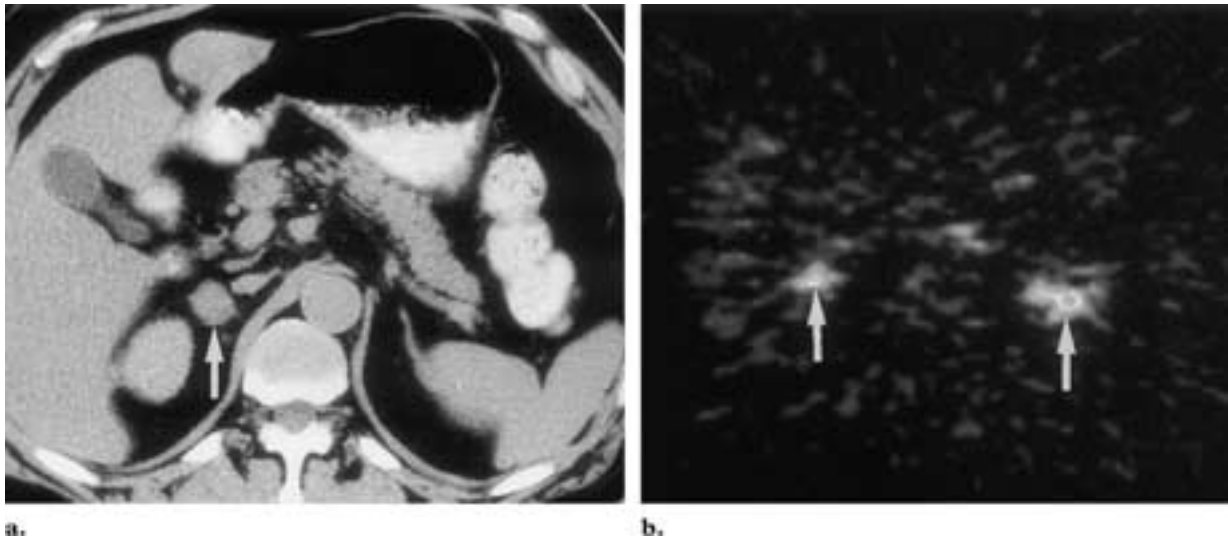


Figure 18. Right adrenal adenoma. (a) Contrast-enhanced CT scan demonstrates a smooth-margin, low-attenuation right adrenal mass (arrow). (b) FDG PET scan shows normal activity in the kidneys (arrows) but no increasing activity in the right adrenal gland.

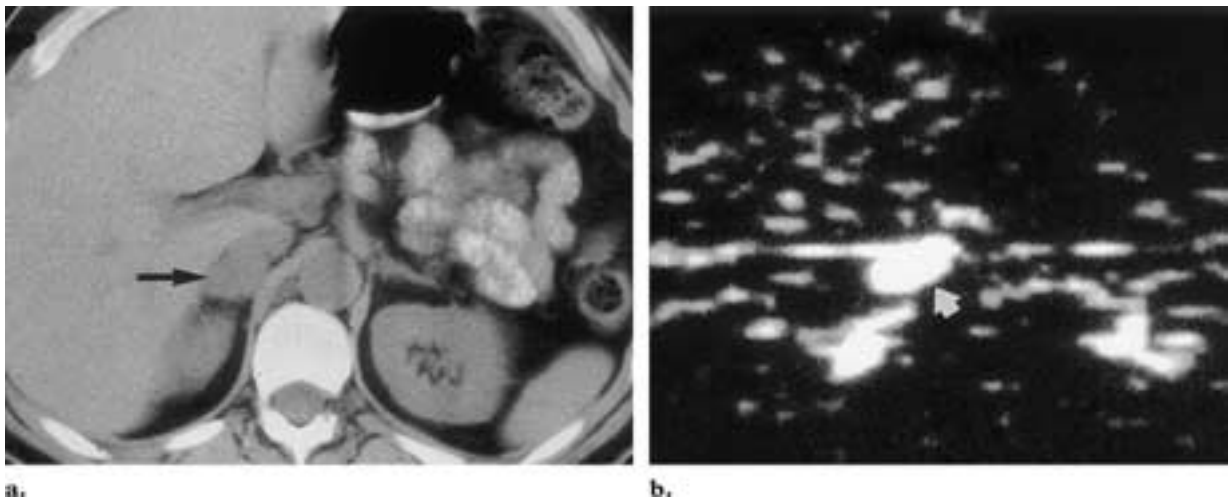


Figure 19. Right adrenal metastasis in a patient with lung carcinoma. (a) Nonenhanced CT scan demonstrates a right adrenal mass (arrow). (b) FDG-PET SPECT scan obtained at the same level shows increased activity in the right adrenal gland (arrow), a finding diagnostic of a metastasis.

80%–100% specificity for differentiating malignant from benign adrenal masses (51–53). If these results are corroborated, FDG PET could become part of the routine evaluation of the patient with a nonhyperfunctioning adrenal mass, especially since the study allows simultaneous whole-body imaging. PET may also be useful for localizing pheochromocytomas (54).

Adrenal Biopsy

Adrenal biopsy is the standard for diagnosis of adrenal pathologic conditions. When adrenal lesions cannot be accurately characterized with CT, MR imaging, or PET, adrenal biopsy should be performed to establish a definitive diagnosis.

Adrenal biopsies are safe procedures with a high degree of accuracy (83%–96%) and a low

complication rate (3%) (55,56). CT is the modality of choice for guiding adrenal biopsies. In general, coaxial technique with a cutting core needle is useful, since many passes can be made through a single outer needle. Because of the proximity of the adrenal gland to the diaphragm, placing the patient in the prone position may cause increased ventilation of the lower lobes and inferior migration of the diaphragm. For this reason, we prefer to perform adrenal biopsies with the patient in the decubitus position with the ipsilateral side down. This position reduces ventilation of the dependent lung, which causes superior movement of the diaphragm, thus lessening the chance for a pneumothorax (Fig 20). In some patients, angling the gantry of the CT scanner allows one to choose a path that avoids the lung parenchyma (Fig 21). In rare cases, a

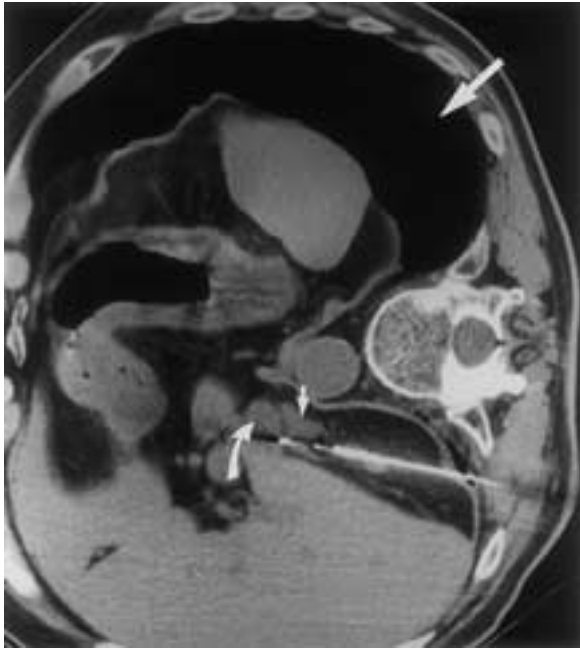
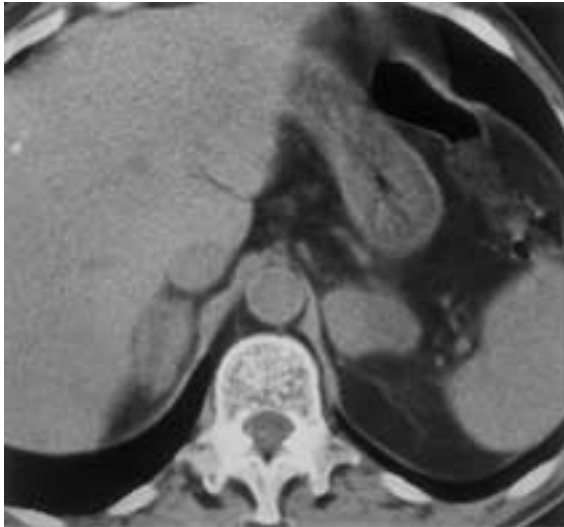
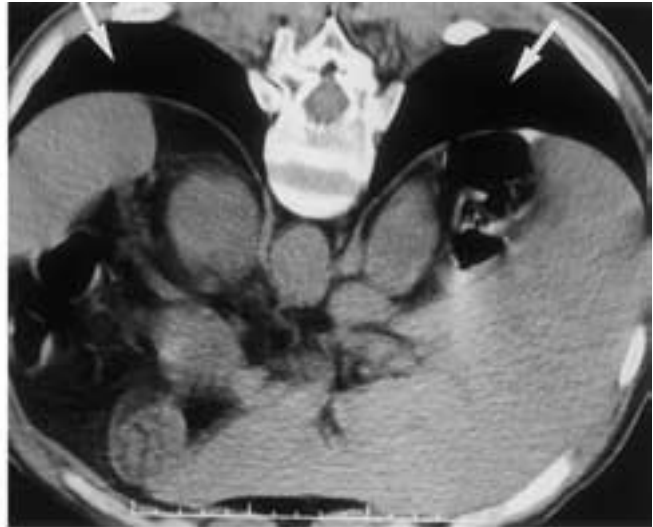


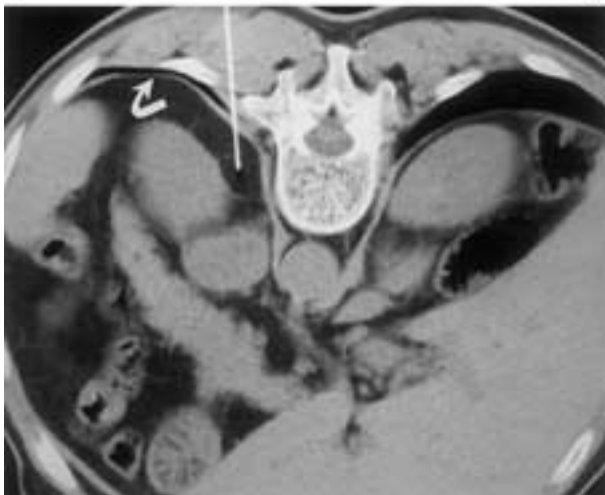
Figure 20. Decubitus position for a right adrenal biopsy in a 76-year-old man with metastatic lung carcinoma. Use of the decubitus position causes decreased ventilation of the dependent lung, allowing a larger window for access to the adrenal gland. As seen on the CT scan, the nondependent lung has markedly increased aeration (large straight arrow) compared with the dependent lung. In addition, use of a coaxial core biopsy system allows access to the adrenal gland (small arrow) while avoiding the adjacent inferior vena cava (curved arrow).



a.



b.



c.

Figure 21. Use of an angled gantry for adrenal biopsy in a 64-year-old patient with metastatic lung carcinoma. (a) Nonenhanced diagnostic CT scan obtained with the patient in the supine position demonstrates bilateral adrenal masses. (b) CT scan acquired with the patient in the prone position shows increased aeration of the lung bases (arrows), which makes access to the adrenal glands difficult. (c) With the CT gantry angled 20° and the patient in the prone position, the radiologist has a safer route of access to the left adrenal gland without transgressing a significant amount of pulmonary parenchyma (arrow).

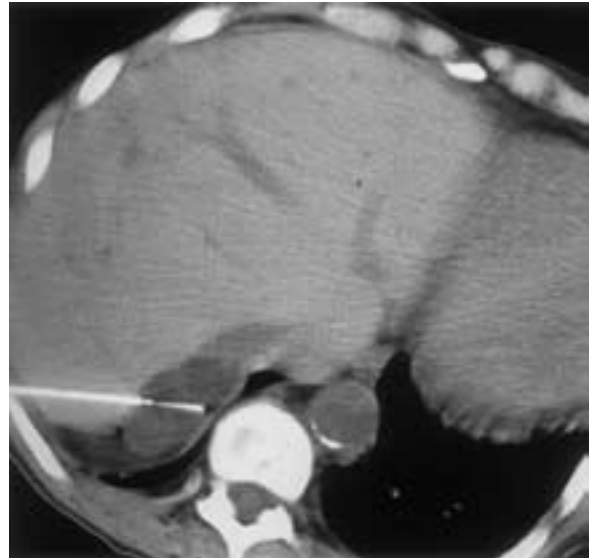


Figure 22. Transhepatic approach to right adrenal biopsy in a 69-year-old woman with breast cancer. CT scan shows the biopsy needle placed through the liver.

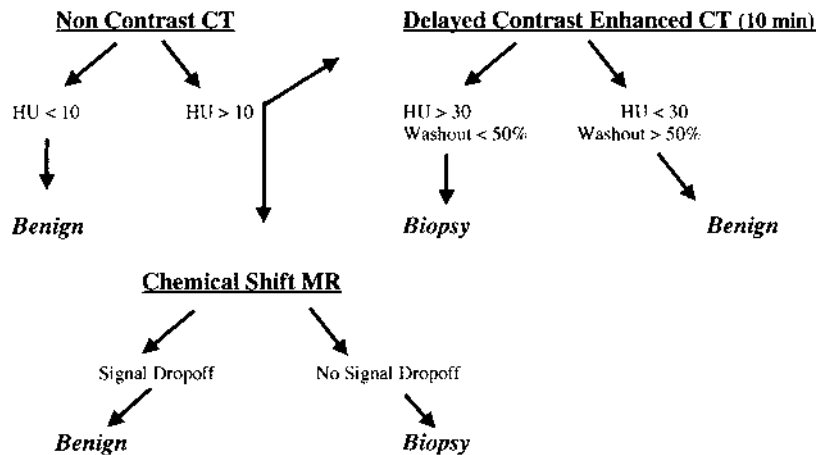


Figure 23. Algorithm summarizes the work-up used to differentiate benign from malignant adrenal masses in oncology patients.

decubitus position or an angled gantry may not allow safe access to the right adrenal gland. For these patients, a transhepatic approach may be used, guided either by US or CT (Fig 22).

Adrenal biopsy is a safe and reliable technique for providing definitive diagnosis in patients in whom accurate staging is mandatory. A summary algorithm of the work-up of an enlarged adrenal gland in the oncologic patient is presented in Figure 23.

Miscellaneous Diseases Affecting the Adrenal Gland

Addison disease is the sequela of adrenal gland hypofunction in which over 90% of the gland is destroyed. Tuberculosis is the most common cause of Addison disease worldwide, but an auto-

immune abnormality is the most common cause in developed countries. In Addison disease from an autoimmune abnormality, the adrenal gland is small at CT (57). A second cause of Addison disease is replacement of the adrenal gland by either neoplasm, hemorrhage, or infection. In these instances, the adrenal gland is often enlarged (58). The adrenal masses caused by granulomatous disease or hemorrhage may involute and subsequently calcify (Fig 24). Addison disease is a clinical diagnosis based on clinical and biochemical findings, not one that is reliably established by imaging methods.

Adrenal carcinoma is a rare adrenal neoplasm arising from the cortex and is bilateral in 10% of patients (59). Fifty percent of adrenal carcinomas are functioning neoplasms with secondary sequelae from the hormone produced, such as Cushing, virilization, feminization, or Conn syndromes. Adrenal carcinomas are usually large at presentation, ranging from 4 to 10 cm, and het-

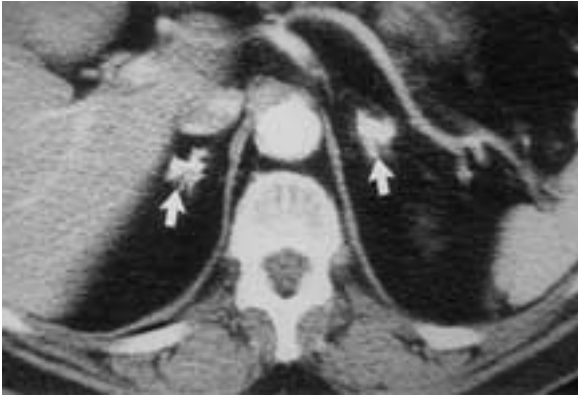


Figure 24. Addison disease in a 51-year-old man. Contrast-enhanced CT scan shows both adrenal glands, which appear small and with dense calcification. The cause of the calcification was not known but may have been due to remote hemorrhage or tuberculosis.

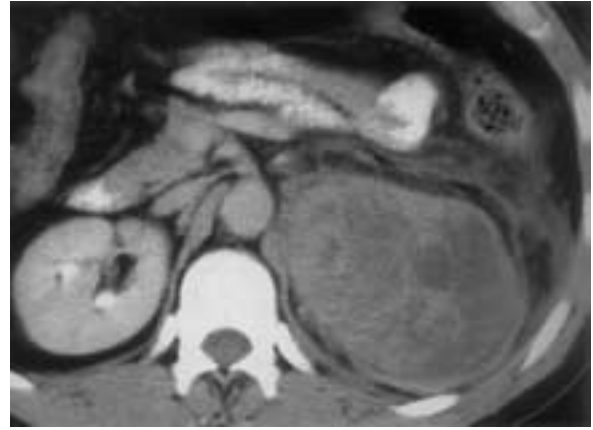


Figure 25. Adrenal carcinoma in a patient who presented with left flank pain. Contrast-enhanced CT scan demonstrates an 11-cm necrotic mass in the left adrenal gland, which causes inferior displacement of the left kidney. There is stranding of the adjacent retroperitoneal fat.



Figure 26. Bilateral myelolipomas in a 79-year-old man. Nonenhanced CT scan shows an exophytic mass of fat attenuation (straight arrow) in the right adrenal gland. The left adrenal gland has a soft-tissue mass containing calcifications and a central area of fat attenuation (curved arrow). These benign adrenal lesions were stable over 4 years.

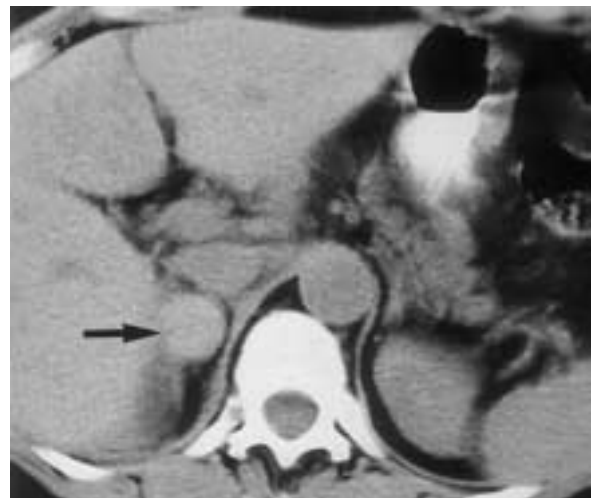


Figure 27. Right adrenal hemorrhage in a 57-year-old woman who sustained pelvic trauma in a motor vehicle accident. Nonenhanced helical CT scan of the abdomen obtained 2 days after the accident demonstrates an enlarged right adrenal mass (arrow). The mass was not present on CT scans acquired at admission (not shown). The attenuation of the right adrenal hemorrhage was 53 HU.

erogeneous (Fig 25). They commonly have central necrosis, and calcification has been described in 30% of cases.

Myelolipomas are rare benign tumors estimated to occur in 0.2%–0.4% of the population based on autopsy series (60,61). These tumors are composed of myeloid, erythroid, and fatty elements and occasionally calcify. The imaging appearance of myelolipomas is based on the fat content of the lesion; thus, they appear echogenic at US, low attenuation at CT, and hyperintense on T1-weighted in-phase MR images. The presence of pure fat within an adrenal lesion at CT is diagnostic of a myelolipoma, and no further work-up is required (Fig 26).

Adrenal hemorrhage results from trauma, systemic anticoagulation therapy, sepsis, or stress such as surgery (62). Trauma accounts for 80% of cases of adrenal hemorrhage. Bilateral hemorrhage occurs in 20% of cases, and adrenal insufficiency secondary to hemorrhage is extremely unusual. At CT, acute adrenal hemorrhage has increased attenuation (Fig 27). Adrenal hemorrhage also has a typical appearance at MR imaging, with T1 hyperintensity secondary to methemoglobin and a T2 dark rim along the periphery

for chronic adrenal hemorrhage due to hemosiderin-laden macrophages. The MR imaging appearance depends on the age of the hemorrhage, which may be divided into acute and chronic based on the imaging findings (63).

Lymphoma of the adrenal gland is unusual, and non-Hodgkin lymphoma is the most common subtype. The literature reports a 4% incidence of adrenal involvement in patients with non-Hodgkin lymphoma (64). Adrenal lymphoma is bilateral in 50% of the cases and is usually associated with retroperitoneal adenopathy or other sites of metastases (Fig 28).

Adrenal cysts are rare entities with typical imaging findings at CT and MR imaging (65). These lesions usually have low attenuation at CT, and there may be wall enhancement with administration of intravenous contrast material. The wall may also contain thin calcification. These lesions are typically hypointense on T1-weighted images and hyperintense on T2-weighted images. Cysts may be derived from the endothelium in 45% of cases, result from pseudocysts from prior hemorrhage in 39%, or result from parasitic diseases such as echinococcosis in less than 10%. In an asymptomatic patient, adrenal cysts should be followed up with sequential imaging studies to assure stability and exclude metastatic disease.

Tuberculosis, histoplasmosis, and blastomycosis can involve the adrenal gland. Typically, these infections result in bilateral enlargement of the adrenal glands. In chronic cases, the glands may atrophy and calcify. Extensive involvement by these organisms may result in adrenal insufficiency.

Summary

There has been a large amount of recent research discussing the evolving role of radiology in both detecting and characterizing abnormalities of the adrenal gland. The role of CT has continued to expand in both detection and characterization of an adrenal mass. For a suspected hyperfunctioning adrenal neoplasm, CT should be performed after the appropriate biochemical screening examinations have been performed. To differentiate a benign adenoma from a metastasis in the oncology patient, nonenhanced CT should be performed and attenuation of the mass quantified. If the attenuation of the adrenal mass is 10 HU or less, the mass is an adenoma and the work-up can stop. If the attenuation is over 10 HU, contrast-enhanced CT should be performed and washout calculated. A washout of over 50% implies an adenoma. If the mass remains indeterminate, MR

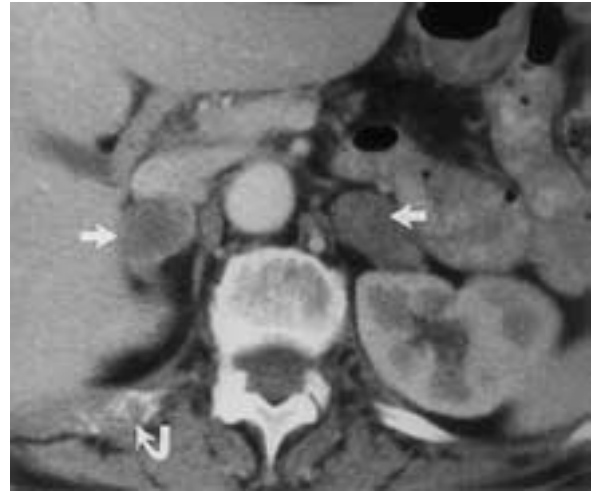


Figure 28. Adrenal lymphoma in a 74-year-old woman with biopsy-proved non-Hodgkin lymphoma. Contrast-enhanced CT scan demonstrates bilateral adrenal masses (straight arrows). The patient also has a destructive lesion from the lymphoma in the right rib (curved arrow).

imaging or adrenal biopsy should be performed. Finally, certain features can be used by the radiologist to establish a definitive diagnosis for an adrenal mass based on imaging findings alone.

References

1. Abrams HL, Siegelman SS, Adams DF, et al. Computed tomography versus ultrasound of the adrenal gland: a prospective study. *Radiology* 1982; 143:121-128.
2. Witteles RM, Kaplan EL, Roizen MF. Sensitivity of diagnostic and localization tests for pheochromocytoma in clinical practice. *Arch Intern Med* 2000; 160:2521-2524.
3. Bravo EL, Gifford RW. Current concepts: pheochromocytoma—diagnosis localization and management. *N Engl J Med* 1984; 311:1298-1303.
4. Siperstein AE, Berber E, Engle KL, Duh QY, Clark OH. Laparoscopic posterior adrenalectomy: technical considerations. *Arch Surg* 2000; 135: 967-971.
5. Krebs TL, Wagner BJ. MR imaging of the adrenal gland: radiologic-pathologic correlation. *RadioGraphics* 1998; 18:1425-1440.
6. Varghese JC, Hahn PF, Papanicolau N, Mayo-Smith WW, Gaa JA, Lee MJ. MR differentiation of pheochromocytoma from other adrenal lesions based on qualitative analysis of T2 relaxation times. *Clin Radiol* 1997; 52:603-606.
7. Shapiro B, Copp JE, Sisson JC, Eyre PL, Wallis J, Beierwaltes WH. Iodine-131 metaiodobenzylguanidine for the locating of suspected pheochromocytoma: experience in 400 cases. *J Nucl Med* 1985; 26:576-585.
8. Maurea S, Cuocolo A, Reynolds JC, et al. Iodine-131-metaiodobenzylguanidine scintigraphy in preoperative and postoperative evaluation of paragangliomas: comparison with CT and MRI. *J Nucl Med* 1993; 34:173-179.
9. Freitas JE. Adrenal cortical and medullary imaging. *Semin Nucl Med* 1995; 25:235-250.

10. Krenning EP, Kwekkeboom DJ, Pauwels S, Kvols LK, Reubi JC. Somatostatin receptor scintigraphy. In: Freeman LM, ed. *Nuclear Medicine Annual* 1995. New York, NY: Raven, 1995; 1–50.
11. Dallman MF, Akana SF, Levin N, et al. Corticosteroids and the control of function in the hypothalamo-pituitary-adrenal (HPA) axis. *Ann N Y Acad Sci* 1994; 746:22–31.
12. Sohaib SA, Hanson JA, Newell-Price JDC, et al. CT appearance of the adrenal glands in adrenocorticotrophic hormone-dependent Cushing's syndrome. *AJR Am J Roentgenol* 1999; 172:997–1002.
13. Kaye TB, Crapo L. The Cushing syndrome: an update on diagnostic tests. *Ann Intern Med* 1990; 112:434–444.
14. Freitas JE, Herwig KR, Cerny JC, Beierwaltes WH. Preoperative localization of adrenal remnants. *Surg Gynecol Obstet* 1977; 145:705–708.
15. Dunnick NR. Adrenal imaging: current status. *AJR Am J Roentgenol* 1990; 154:927–936.
16. Dunnick NR, Leight GS, Robidoux MA, Leder RA, Paulson E, Kurylo L. CT in the diagnosis of primary aldosteronism: sensitivity in 29 patients. *AJR Am J Roentgenol* 1993; 160:321–324.
17. Ikeda DM, Francis IR, Glazer GM, Amendola MA, Gross MD, Aisen AM. The detection of adrenal tumors and hyperplasia in patients with primary aldosteronism: comparison of scintigraphy, CT and MR imaging. *AJR Am J Roentgenol* 1989; 153:301–306.
18. Glazer HS, Weyman PJ, Sagal SS, Levitt RG, McClennan BL. Adrenal masses: incidental discovery on computed tomography. *AJR Am J Roentgenol* 1982; 139:81–85.
19. Dunnick NR, Korobkin M, Francis I. Adrenal radiology: distinguishing benign from malignant masses. *AJR Am J Roentgenol* 1996; 167:861–867.
20. Abrams HL, Spiro R, Goldstein N. Metastases in carcinoma: analysis of 1000 autopsied cases. *Cancer* 1950; 3:74–85.
21. Francis IR, Smid A, Gross MD, Shapiro B, Naylor B, Glazer GM. Adrenal masses in oncologic patients: function and morphologic evaluation. *Radiology* 1988; 166:353–356.
22. Korobkin M, Giordano TJ, Brodeur FJ, et al. Adrenal adenomas: relationship between histologic lipid and CT and MR findings. *Radiology* 1996; 200:743–747.
23. Lee MJ, Hahn PF, Papanicolaou N, et al. Benign and malignant adrenal masses: CT distinction with attenuation coefficients, size, and observer analysis. *Radiology* 1991; 179:415–418.
24. Korobkin M, Brodeur FJ, Yutzy GG, et al. Differentiation of adrenal adenomas from nonadenomas using CT attenuation values. *AJR Am J Roentgenol* 1996; 166:531–536.
25. Boland GW, Lee MJ, Gazelle GS, Halpern EF, McNicholas MM, Mueller PR. Characterization of adrenal masses using unenhanced CT: an analysis of the CT literature. *AJR Am J Roentgenol* 1998; 171:201–204.
26. Caoili EM, Korobkin M, Francis IR, Cohan RH, Dunnick NR. Delayed enhanced CT of lipid poor adrenal adenomas. *AJR Am J Roentgenol* 2000; 175:1411–1415.
27. Pena CS, Boland GW, Hahn PF, Lee MJ, Mueller PR. Characterization of indeterminate (lipid-poor) adrenal masses: use of washout characteristics at contrast-enhanced CT. *Radiology* 2000; 217:798–802.
28. Korobkin M, Brodeur FJ, Francis IR, Quint LE, Dunnick NR, Goodsitt M. Delayed enhanced CT for differentiation of benign from malignant adrenal masses. *Radiology* 1996; 200:737–742.
29. Szolar DH, Kammerhuber FH. Quantitative CT evaluation of adrenal gland masses: a step forward in the differentiation between adenomas and nonadenomas? *Radiology* 1997; 202:517–521.
30. Boland GW, Hahn PF, Pena C, Mueller PR. Adrenal masses: characterization with delayed contrast-enhanced CT. *Radiology* 1997; 202:693–696.
31. Korobkin M, Brodeur FJ, Francis IR, Quint LE, Dunnick NR, Londy F. CT time-attenuation washout curves of adrenal adenomas and nonadenomas. *AJR Am J Roentgenol* 1998; 170:747–752.
32. Szolar DH, Kammerhuber FH. Adrenal adenomas and nonadenomas: assessment of washout at delayed contrast-enhanced CT. *Radiology* 1998; 207:369–375.
33. Krestin GP, Friedmann G, Fishbach R, Neufant KFR, Allolio B. Evaluation of adrenal masses in oncologic patients: dynamic contrast-enhanced MR vs CT. *J Comput Assist Tomogr* 1991; 15: 104–110.
34. Ichikawa T, Ohtomo K, Uchiyama G, Fujimoto H, Nasu K. Contrast-enhanced dynamic MRI of adrenal masses: classification of characteristic enhancement patterns. *Clin Radiol* 1995; 50:295–300.
35. Mitchell DG, Crovello M, Matteucci T, Peterson RO, Miettinen MM. Benign adrenocortical masses: diagnosis with chemical shift MR imaging. *Radiology* 1992; 185:345–351.
36. Reinig JW, Stutley JE, Leonhardt CM, Spicer KM, Margolis M, Caldwell CB. Differentiation of adrenal masses with MR imaging: comparison of techniques. *Radiology* 1994; 192:41–46.
37. Schwartz LH, Panicek DM, Louthcer JA, et al. Adrenal masses in patients with malignancy: prospective comparison of echo-planar, fast spin-echo and chemical-shift MR imaging. *Radiology* 1995; 197:421–425.
38. Lee MJ, Mayo-Smith WW, Hahn PF, et al. State-of-the-art MR imaging of the adrenal gland. *RadioGraphics* 1994; 14:1015–1029.
39. Semelka RC, Shoenut JP, Lawrence PH, et al. Evaluation of adrenal masses with gadolinium enhancement and fat-suppressed MR imaging. *J Magn Reson Imaging* 1993; 3:337–343.
40. Chezmar JL, Robbins SM, Nelson R, Steinberg HV, Torres WE, Bernardino ME. Adrenal masses: characterization using MR imaging. *Radiology* 1988; 166:357–359.
41. Outwater EK, Siegelman ES, Huang AB, Birnbaum BA. Adrenal masses: correlation between CT attenuation value and chemical shift ratio at MR imaging with in-phase and opposed-phase sequences. *Radiology* 1996; 200:749–752. [Erratum: *Radiology* 1996; 201:880]
42. Mayo-Smith WW, Lee MJ, McNicholas MM, Hahn PF, Boland GW, Saini S. Characterization of adrenal masses (<5 cm) by use of chemical shift

- MR imaging: observer performance versus quantitative measures. *AJR Am J Roentgenol* 1995; 165:91-95.
43. Bilbey JH, McLoughlin RF, Kurkjian PS, et al. MR imaging of adrenal masses: volume of chemical-shift imaging for distinguishing adenomas from other tumors. *AJR Am J Roentgenol* 1995; 164:637-642.
 44. Outwater EK, Siegelman ES, Radecki PD, Piccoli CW, Mitchell DG. Distinction between benign and malignant adrenal masses: value of T1-weighted chemical-shift MR imaging. *AJR Am J Roentgenol* 1995; 165:579-583.
 45. Korobkin M, Lombardi TJ, Aisen AM, et al. Characterization of adrenal masses with chemical-shift and gadolinium-enhanced MR imaging. *Radiology* 1995; 197:411-418.
 46. Tsushima Y, Ishizaka H, Matsumoto M. Adrenal masses: differentiation with chemical-shift, fast low-angle shot MR imaging. *Radiology* 1993; 186:705-709.
 47. Heinz-Peer G, Honigschnabl S, Schneider B, Niederle B, Kaserer K, Lechner G. Characterization of adrenal masses using MR imaging with histopathologic correlation. *AJR Am J Roentgenol* 1999; 173:15-22.
 48. Schwartz LH, Macari H, Huvos AG, Panicek DM. Collision tumors of the adrenal gland: demonstration and characterization on MR imaging. *Radiology* 1996; 201:757-760.
 49. McNicholas MM, Lee MJ, Mayo-Smith WW, Hahn PF, Boland GW, Mueller PR. An imaging algorithm for the differential diagnosis of adrenal adenomas and metastases. *AJR Am J Roentgenol* 1995; 165:1453-1459.
 50. Schwartz LH, Ginsberg MS, Burt ME, et al. MRI as an alternative to CT-guided biopsy of adrenal masses in patients with lung cancer. *Ann Thorac Surg* 1998; 65:193-197.
 51. Boland GW, Goldberg MA, Lee MJ, et al. Indeterminate adrenal mass in patients with cancer: evaluation at PET with 2-[F-18]-fluoro-2-deoxy-D-glucose. *Radiology* 1995; 194:131-134.
 52. Erasmus JJ, Patz EF Jr, McAdams HP, et al. Evaluation of adrenal masses in patients with bronchogenic carcinoma using 18F-fluorodeoxyglucose positron emission tomography. *AJR Am J Roentgenol* 1997; 168:1357-1360.
 53. Maurea S, Mainolfi C, Bazzicalupo L, et al. Imaging of adrenal tumors using FDG PET: comparison of benign and malignant lesions. *AJR Am J Roentgenol* 1999; 173:25-29.
 54. Shulkin BL, Thompson NW, Shapiro B, Francis IR, Sisson JC. Pheochromocytomas: imaging with 2-[fluorine-18]fluoro-2-deoxy-D-glucose PET. *Radiology* 1999; 212:35-41.
 55. Welch TJ, Sheedy PF II, Stephens DH, Johnson CM, Swensen SJ. Percutaneous adrenal biopsy: review of a 10-year experience. *Radiology* 1994; 193:341-344.
 56. Silverman SG, Mueller PR, Pinkney LP, Koenker RM, Seltzer SE. Predictive value of image-guided adrenal biopsy: analysis of results of 101 biopsies. *Radiology* 1993; 187:715-718.
 57. Doppman JL, Gill JR Jr, Nienhuis AW, Earll JM, Long JA Jr. CT findings in Addison's disease. *J Comput Assist Tomogr* 1982; 6:757-761.
 58. Kawashima A, Sandler CM, Fishman EK, et al. Spectrum of CT findings in nonmalignant disease of the adrenal gland. *RadioGraphics* 1998; 18:393-412.
 59. Pommier RF, Brennan MF. An eleven-year experience with adrenocortical carcinoma. *Surgery* 1992; 112:963-971.
 60. Kenney PJ, Wagner BJ, Rao P, Heffess CS. Myelolipoma: CT and pathologic features. *Radiology* 1998; 208:87-95.
 61. Otal P, Escourrou G, Mazerolles C, et al. Imaging features of uncommon adrenal masses with histopathologic correlation. *RadioGraphics* 1999; 19:569-581.
 62. Burks DW, Mirvis SE, Shanmuganathan K. Acute adrenal injury after blunt abdominal trauma: CT findings. *AJR Am J Roentgenol* 1992; 158:503-507.
 63. Kawashima A, Sandler CM, Ernst RD, et al. Imaging of nontraumatic hemorrhage of the adrenal gland. *RadioGraphics* 1999; 19:949-963.
 64. Glazer HS, Lee JKT, Balfe DM, Mauro MA, Griffith R, Sagel SS. Non-Hodgkin lymphoma: computed tomographic demonstration of unusual extranodal involvement. *Radiology* 1983; 149:211-217.
 65. Tung GA, Pfister RC, Papanicolaou N, Yoder IC. Adrenal cysts: imaging and percutaneous aspiration. *Radiology* 1989; 173:107-110.